IL NUOVO CIMENTO Vol. 37 C, N. 4 Luglio-Agosto 2014
DOI 10.1393/ncc/i2014-11794-2

Communications: SIF Congress 2012

Revealing the electronic band structure of trilayer graphene on SiC(*)

C. Coletti(**)

Center for Nanotechnology Innovation @ NEST, Istituto Italiano di Tecnologia
Piazza San Silvestro 12, I-56127 Pisa, Italy and
Max-Planck-Institut für Festkörperforschung - Heisenbergstr. 1, D-70569 Stuttgart, Germany

ricevuto il 9 Gennaio 2014; approvato il 16 Marzo 2014

Summary. — Recently, a great deal of attention has been devoted to trilayer graphene because it displays stacking and electric-field–dependent electronic properties well-suited for electronic and photonic applications. Several theoretical studies have predicted the electronic dispersion of Bernal (ABA) and rhombohedral (ABC) stacked trilayers. However, a direct experimental visualization of a well-resolved band structure has not yet been reported. In this work, angle resolved photoemission spectroscopy data which show with high resolution the electronic band structure of trilayer graphene on 6H-SiC(0001) are presented. Electronic bands obtained from tight-binding calculations are fitted to the experimental data to extract the interatomic hopping parameters for Bernal and rhombohedral stacked trilayers. The presented results suggest that on SiC substrates the occurrence of rhombohedral stacked trilayer is significantly higher than in natural bulk graphite.

PACS 73.22.Pr – Electronic structure of graphene.
PACS 81.05.ue – Graphene.
PACS 61.48.Gh – Structure of graphene.

1. – Introduction

In recent times, trilayer graphene (TLG) has attracted wide attention owing to its stacking and electric-field–dependent electronic properties [1-8]. Trilayer graphene has two naturally stable allotropes characterized by either Bernal (ABA) or rhombohedral (ABC) stacking of the individual carbon layers. In ABA-stacking the atoms of the topmost layer obtain lateral positions exactly above those of the bottom layer (fig. 1(a)).

(*) This communication was awarded at the SIF National Congress of Napoli, 2012, but it is herewith published with the communications awarded in 2013.
(**) E-mail: camilla.coletti@iit.it

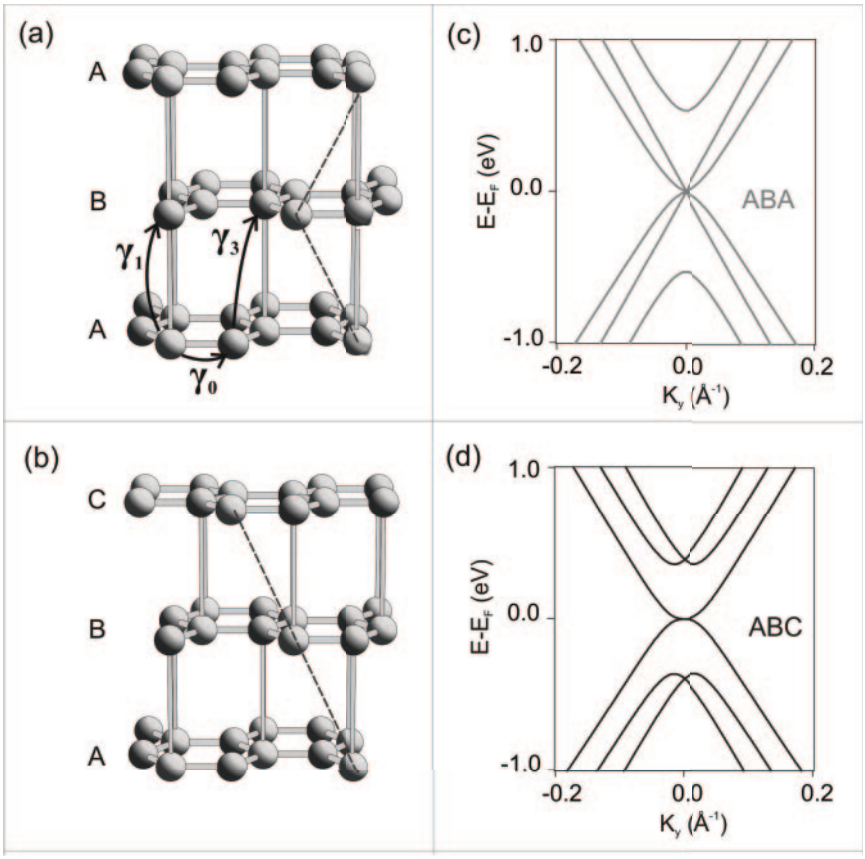

Fig. 1. – (a,b) Schematic representation of the stacking sequence in (a) Bernal and (b) rhombohedral TLG. The interatomic tight-binding hopping parameters between adjacent layers—thus valid for both stackings—are denoted by the black arrows in panel (a). (c,d) Calculated low-energy band structure for Bernal (c) and rhombohedral (d) TLG.

In an ABC-stacked trilayer each layer is laterally shifted with respect to the layer below by a third of the diagonal of the lattice unit cell (fig. 1(b)). Several theoretical studies have predicted the electronic dispersion of ABA- and ABC-stacked trilayers using tight-binding approaches [1-3, 9-13]. The low-energy band structure of ABA TLG consists of a linearly dispersing (monolayer-like) band and bilayer-like quadratically dispersing bands (fig. 1(c)) [1,3,11]. Quite differently, ABC trilayers have a single low-energy band with approximately cubic dispersion (fig. 1(d)) [1-3, 12]. A very intriguing distinction between the two allotropes is their behavior in the presence of a perpendicular electric field: ABA-stacked trilayers are expected to display a tunable band overlap, while ABC-stacked trilayers present a tunable band-gap, the latter being very appealing for electronic applications [3, 10]. However, the alluring rhombohedral phase is quite rare in nature as the energetically favored Bernal stacking makes up for more than 80% of the existing graphite [14, 15].

On the experimental side, progress in revealing the fundamental properties of TLG has been slow as such studies require homogenous trilayers with a well-defined stacking sequence over areas of hundreds of micrometers. Infrared conductivity and transport

measurements have confirmed that a band-gap can be opened in ABC-stacked TLG when applying a perpendicular electric field, while no band-gap has been observed in ABA-stacked trilayers [5]. However, a direct visualization of the electronic band structure of homogenous TLG via angle resolved photoemission spectroscopy (ARPES) has not been reported so far. In 2007, Ohta and colleagues reported ARPES spectra of few-layers graphene on SiC [16]. However, the separation of contributions from areas with different number of layers or different stacking in such a configuration is ambiguous and rather challenging. Clearly, the availability of highly resolved experimental ARPES data for TLG would allow for a direct comparison with the band structure predicted by the tight-binding formalism, thus leading to a precise determination of the interatomic interactions (sketched by the hopping parameters in panel (a)).

In the present paper large-area homogenous TLG is obtained on hexagonal SiC (*i.e.*, 6H-SiC(0001)) by first growing bilayer graphene (BLG) and then adopting the hydrogen intercalation technique described in [17]. The thickness of such samples is confirmed by X-ray photoelectron spectroscopy (XPS). Highresolution ARPES energy-momentum (E-k) maps are acquired for homogeneous TLG samples. These maps correlate well with the band structure calculated by theory for both ABA and ABC stacks. Band structure results obtained from tight-binding calculations [18] are used to fit the experimental ARPES data and to extract the hopping parameters both for ABA- and ABC-stacked trilayers.

2. – Methods

Homogeneous graphene bilayers were grown on nominally on-axis oriented 6H-SiC(0001) substrates. The growth parameters were finely optimized to obtain the highest bilayer coverage. Growth was performed in an inductively heated furnace at a temperature of 1350 °C, a pressure of 10^{-5} mbar for 1 hour [19]. H-intercalation was performed by annealing the samples for 20 to 40 minutes in a hydrogen atmosphere at a pressure of 830 mbar and a temperature of 1000 °C. The thickness of the samples was evaluated via XPS using the photons from a non-monochromatic Mg $K\alpha$ source ($h\nu = 1253.6$ eV). The electronic dispersion was investigated via ARPES at the end-station of the SIS beamline at the Swiss Light Source synchrotron facility using p-polarized light. The spectra and the costant energy maps (CEMs) reported were measured with a photon energy of 90 eV.

3. – Results

A characteristic XPS spectrum for as-grown BLG on 6H-SiC(0001) is displayed in the top part of fig. 2. The raw data (black dots) can be fitted with four components. The broader dominant peak at 283.9 eV is the SiC (bulk) related component while the narrower peak at 284.7 eV is the graphene related component. The components labeled S1 and S2 centered at 285 eV and 285.6 eV, respectively, are the signature of the interface layer known as zerolayer or buffer layer [17,20]. Relative intensity of the graphene component with respect to the SiC one confirms that the sample is bilayer graphene. Moreover, low-energy electron microscopy (LEEM) measurements performed on the sample used in this work and reported in [18] demonstrate its high homogeneity; *i.e.*, the bilayer domains occupy more than 80% of the overall area. The band structure of the sample was measured around the $\overline{\mathrm{K}}$-point of the graphene Brillouin zone (BZ) using synchrotron-radiation–based ARPES. The spectrum shown in fig. 3(a) is representative of the entire area of the sample. The spectrum is extremely sharp and exclusively consists of parabolic

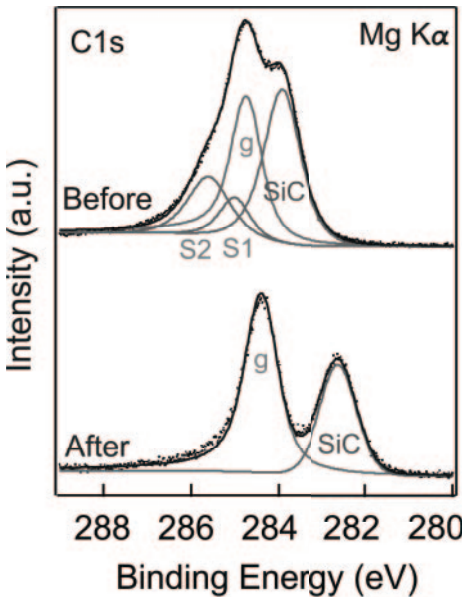

Fig. 2. – C1s spectra of as-grown bilayer graphene on 6H-SiC(0001) before (top) and after (bottom) hydrogen intercalation. The raw data is plotted as black dots and the envelope of the fitted components (described in the text) as a continuous line. The absence of the interface S1 and S2 components and the increased intensity of the graphene peak in the bottom spectrum confirm that after intercalation the sample has turned into a quasi-free standing trilayer.

bands, the signature of bilayer graphene, corroborating the extreme homogeneity of the graphene film. Hence, the graphene thickness is essentially constant over a large area (the spot-size of the UV light beam is about $100 \times 50\,\mu\text{m}^2$) and the small percentage of domains of different thickness does not cause significant contributions to the measured band structure. In fig. 3(d), theoretical bands obtained by tight-binding calculations for a Bernal stacked bilayer using the formalism of McCann and Fal'ko [21] are fitted to the experimental data. As expected for epitaxial BLG on SiC, the Fermi level is shifted by around 0.3 eV above the Dirac energy of the π-bands—indicative of n-type doping [22-24]. Also, the characteristic band-gap of ~ 120 meV caused by the electrostatic asymmetry of the bilayer slab on the SiC substrate is visible [23, 24]. The bottom XPS spectrum in fig. 2 was collected after annealing the bilayer sample in hydrogen. As described in [17, 25], this treatment causes hydrogen to intercalate between the buffer layer and the SiC(0001) surface. Hydrogen atoms passivate the Si dangling bonds, so that the overlaying graphene layers are electronically and structurally decoupled from the SiC substrate. In this way, the buffer layer becomes an electronically active monolayer and, more generally, a n-layer graphene film transforms into a $(n + 1)$-layer graphene film. Indeed, as expected after a successful hydrogen intercalation process, the SiC related component shifts to about 282.6 eV, while the graphene related component, now more intense, is found at 284.4 eV. The total shift of the SiC component is larger than 1 eV, which confirms the presence of hydrogen atoms passivating the Si dangling bonds and causing a respective band bending. Moreover, the increase in intensity of the graphene component together with the complete absence of the interface layer components is ev-

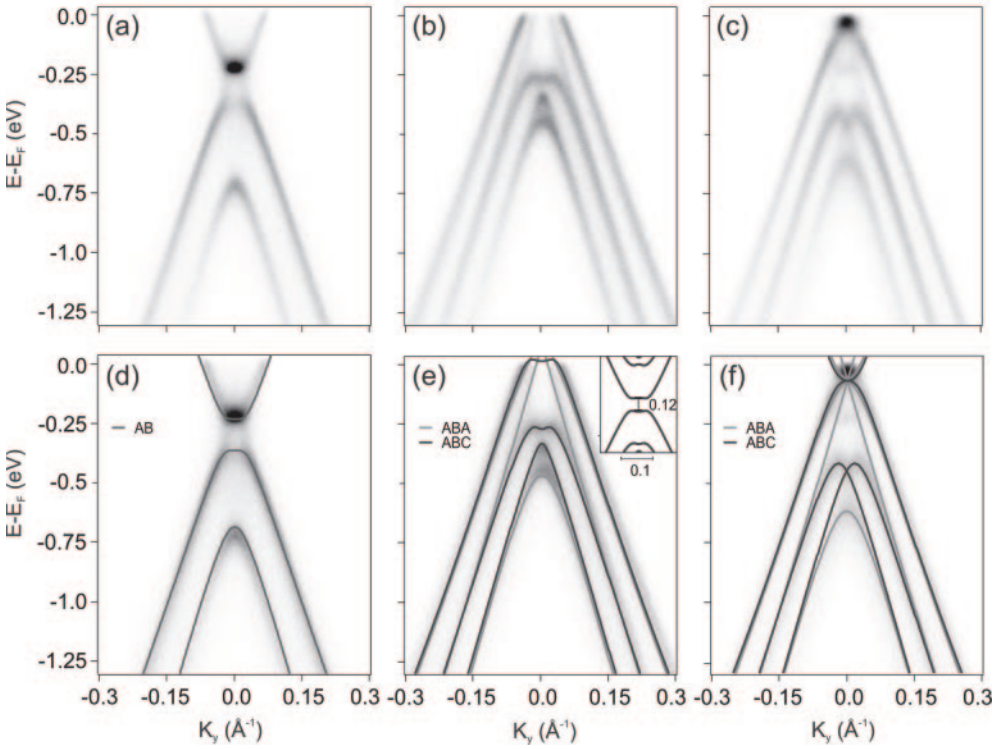

Fig. 3. – Dispersion of the π-bands measured via ARPES for as-grown BLG on 6H-SiC(0001) (a), QFTLG annealed at 400 °C (b) and at about 800 °C (c). The spectra are measured with a photon energy of 90 eV and with scans oriented perpendicular to the $\overline{\Gamma K}$ direction of the graphene Brillouin zone. (d–f) Tight-binding bands fitted to the experimental data shown in (a), (b) and (c), respectively. The fitting retrieves a band-gap in the ABC dispersion in panel (b) of ~ 120 meV (inset in panel (e)) [18].

idence of the fact that BLG has turned—after hydrogen intercalation—into quasi-free standing trilayer graphene (QFTLG).

From this sample we have acquired the first well-resolved direct visualization of the electronic band structure of TLG as displayed in fig. 3(b). The spectrum shown was collected after outgassing the sample at 400 °C, a temperature sufficient to remove air contamination but well below the onset of hydrogen desorption [25]. A mixture of several sharp bands can be observed. The high quality of the measured band structure allows for a precise identification of the trilayer stacking sequence. To this end, theoretical bands derived from tight-binding Hamiltonians describing the ABA and ABC trilayers were fit to the experimental data [18]. Panel (e) shows the results of the fitting procedure superimposed to the electronic dispersions obtained experimentally. The two stacking sequences, ABA and ABC, can be clearly distinguished as indicated by the respective light gray and dark gray fitting curves. The accurate overlap of the calculated bands with the experimental data reveals unambiguously that QFTLG on SiC contains domains of both Bernal and rhombohedral stacking, in contrast to natural graphite which typically only features ABA stacking [14, 15]. The excellent fit also indicates that all

TABLE I. – *Hopping parameters for Bernal and rhombohedral stacked TLG on hexagonal SiC substrates directly calculated from tight-binding fits to experimental ARPES data. All values are in eV.*

Stacking	γ_0	γ_1	γ_3
ABC	−2.86	−0.38	−0.24
ABA	−3.05	−0.39	−0.20

experimentally visible bands belong to trilayer graphene, thus corroborating the overall homogeneous graphene thickness. From the fits in panel (e) the Dirac energy can be determined to be about 90 meV above the Fermi energy. The p-type doping is typical for hydrogen intercalated samples on α-SiC [26-28] and has been recently attributed to the spontaneous polarization of the substrate imposed by hexagonal SiC's pyroelectricity [29]. This polarization obviously induces an electrostatic field across the trilayer slab (the on-site Coulomb potential difference between the first and the third layer is calculated to be 0.12 eV) which modifies the band structure of trilayer graphene as described in [3, 10]. In particular, from the fits it can be derived that at the $\overline{K}$ point an energy band-gap of $\sim 120 \pm 25$ meV is induced (inset in panel (e)) [18]. This value indeed is in agreement with results from infrared conductivity measurements [5]. As reported in refs. [17, 25], by annealing a quasi-free standing monolayer graphene (QFMLG) sample at higher temperatures it is possible to achieve charge neutrality within a few meV. This is also successful for the present QFTLG sample. The band structure shown in panel (c) was measured after prolonged annealing at about 800 °C, which is a higher temperature than that needed to obtain charge neutral quasi-free mono- and bilayer graphene [28]. In fact, the sample appears to have acquired a minimal n-doping after this treatment by possibly desorbing an excess of hydrogen from the Si dangling bonds. The visibility of the onset of the conduction band allows one to appreciate the absence of a measurable band-gap. Hence, after annealing and in consequence retrieving charge neutrality, no on-site Coloumb potential difference is necessary for the calculated bands to be superimposed onto the experimental data in panel (f).

Notably, a simple visual inspection suggests that the intensities of the ABC bands of all the measured spectra are higher than those of the ABA contributions. Detailed analysis of the intensities of the momentum distribution curves (MDCs) is presented in ref. [18] and quantitatively confirms that the ABC branches are significantly more intense than the ABA ones. Of course, it must be taken into consideration that the photoemission intensity of single ABA and ABC branches is expected to vary as a consequence of varying strength and direction of interatomic interactions [16, 30]. Nevertheless, these results suggest that the ABC type of stacking occurs in QFTLG on SiC with a significantly higher incidence than in nature. The tendency of graphene to form on SiC in ABC-stacking could be explained by a weakening of the γ_5 interatomic interaction—a major contributor to the stability of the ABA stacking—due to the displacement of carbon atoms in the buffer layer during the growth process [31].

The hopping parameters obtained from fitting the experimental spectra with theoretical bands derived from tight-binding Hamiltonians describing the ABA and ABC trilayers [18] are listed in table I. The absolute values obtained for γ_0 and γ_1 agree well with those predicted by theory [2, 10, 11, 13] and experimentally retrieved for few layer

graphene and graphite [5, 16, 32]. By comparing experimental and theoretical constant energy maps (CEMs) it is possible to extract the sign of the interlayer coupling parameter γ_1 and the relative sign between γ_1 and γ_3. By adopting this procedure we found that $\gamma_1 < 0$ and $\gamma_3 < 0$ for both stacking arrangements [18]. It should be noted that, although the sign of γ_1 has a directly observable effect on the ARPES bands, up to now it has often been assumed to be positive [2,5,10,11,13,16,32]. As suggested in [30], the negative sign should be a natural consequence of the $z \to -z$ asymmetry of the p_z orbitals of carbon. The term γ_3, which defines the strength of the trigonal warping effect, is in agreement with what is predicted by theory and experimentally obtained for graphite [2, 13, 32].

We have recently shown that high-quality QFTLG can also be obtained on 3C-SiC(111) substrates [18]. This is a remarkable accomplishment, considering that until recently even the growth of large area MLG was considered to be a challenge [33]. Also in this case, homogenous BLG was obtained in a quartz tube and subsequently hydrogen intercalated using the same process which has been adopted in the past for hydrogen passivation of cubic SiC surfaces [34] and for hydrogen intercalation of graphene on cubic SiC [33]. The values of the hopping parameters retrieved for TLG on 3C-SiC(111) are quite similar to those reported above for TLG on hexagonal substrates with the exception of γ_0, which is higher for graphene on 3C-SiC(111). From γ_0 we can derive that the band velocity of the rhombohedral QFTLG on 6H-SiC(0001) is about 0.93×10^6 m/s, while on 3C-SiC(111) it is calculated to be about 1.05×10^6 m/s [18]. However, the differences in band velocity arise from a different concentration of scattering centers due to surface morphology and not from the different substrate polytype [18].

4. – Conclusion

This work reports ARPES data that show with high resolution the band structure of Bernal and rhombohedral TLG obtained on 6H-SiC via hydrogen intercalation. Interatomic hopping parameters for both stacking sequences are retrieved from a direct comparison of the experimental electronic bands with theoretical bands obtained from tight-binding calculations. For ABC stacks and in the presence of an electrostatic asymmetry, the existence of a band-gap of about 120 meV is detected. Notably, the presented results suggest that on SiC substrates the occurrence of ABC-stacked TLG is significantly higher than in natural bulk graphite. Hence, growing TLG on SiC might be the answer to the challenge of controllably synthesizing ABC-stacked trilayer—an ideal material for the fabrication of a new class of gap-tunable devices.

* * *

This work was performed in collaboration with: S. Forti, K. V. Emtsev and U. Starke of the Max Planck Institute of Stuttgart, Germany; A. Principi and M. Polini of NEST, Istituto Nanoscienze-CNR and Scuola Normale Superiore, Pisa, Italy; A. A. Zakharov of the MAX-Lab of Lund, Sweden; K. M. Daniels, B. K. Daas and M. V. S. Chandrashekhar of University of South Carolina, Columbia, USA; A. H. MacDonald of University of Texas at Austin, Texas, USA. C.C. acknowledges the Alexander von Humboldt Foundation for financial support. This work was supported by the Deutsche Forschungsgemeinschaft in the framework of the Priority Program 1459 Graphene (Sta315/8-1). Support by the staff at SLS (Villigen, Switzerland) is gratefully acknowledged.

REFERENCES

[1] Min H. and MacDonald A. H., *Prog. Theor. Phys. Suppl.*, **176** (2008) 227.
[2] Zhang F., Sahu B., Min H. and MacDonald A. H., *Phys. Rev. B*, **82** (2010) 035409.
[3] Koshino M., *Phys. Rev. B*, **81** (2010) 125304.
[4] Craciun M. F. *et al.*, *Nat. Nanotechnol.*, **4** (2009) 383.
[5] Lui C. H., Li Z., Mak K. F., Cappelluti E. and Heinz T. F., *Nat. Phys.*, **7** (2011) 944.
[6] Bao W. *et al.*, *Nat. Phys.*, **7** (2011) 948.
[7] Zhang L., Zhang Y., Camacho J., Khodas M. and Zaliznyak I., *Nat. Phys.*, **7** (2011) 953.
[8] Yacoby A., *Nat. Phys.*, **7** (2011) 925.
[9] Guinea F., Castro Neto A. H. and Peres N. M. R., *Phys. Rev. B*, **73** (2006) 245426.
[10] Aoki M. and Amawashi H., *Solid State Commun.*, **142** (2007) 123.
[11] Grüneis A. *et al.*, *Phys. Rev. B*, **78** (2008) 205425.
[12] Koshino M. and McCann E., *Phys. Rev. B*, **80** (2009) 165409.
[13] Avetisyan A. A., Partoens B. and Peeters F. M., *Phys. Rev. B*, **81** (2010) 115432.
[14] Lipson H. and Stokes A. R., *Proc. R. Soc. A*, **101** (1942) 181.
[15] Lui C. H., Li Z., Chen Z., Klimov P. V., Brus L. E. and Heinz T. F., *Nano Lett.*, **11** (2011) 164.
[16] Ohta T. *et al.*, *Phys. Rev. Lett.*, **98** (2007) 206802.
[17] Riedl C., Coletti C., Iwasaki T., Zakharov A. A. and Starke U., *Phys. Rev. Lett.*, **103** (2009) 246804.
[18] Coletti C., Forti S., Principi A., Emtsev K. V., Zakharov A. A., Daniels K. M., Daas B. K., Chandrashekhar M. V. S., Ouisse T., Chaussende D., MacDonald A. H., Polini M. and Starke U., *Phys. Rev. B*, **88** (2013) 155439.
[19] Daas B. K., Daniels K. M., Sudarshan T. S. and Chandrashekhar M. V. S., *J. Appl. Phys.*, **110** (2011) 113114.
[20] Emtsev K. V., Speck F., Seyller T., Ley L. and Riley J. D., *Phys. Rev. B*, **77** (2008) 155303.
[21] McCann E. and Fal'ko V. I., *Phys. Rev. Lett.*, **96** (2006) 086805.
[22] Starke U., Forti S., Emtsev K. V. and Coletti C., *MRS Bull.*, **37** (2012) 1177.
[23] Ohta T., Bostwick A., Seyller T., Horn K. and Rotenberg E., *Science*, **313** (2006) 951.
[24] Coletti C., Riedl C., Lee D. S., Krauss B., von Klitzing K., Smet J. and Starke U., *Phys. Rev. B*, **81** (2010) 235401.
[25] Forti S., Emtsev K. V., Coletti C., Zakharov A. A. and Starke U., *Phys. Rev. B*, **84** (2011) 125449.
[26] Coletti C., Forti S., Emtsev K. V. and Starke U., *Carbon Nanostructures*, in *GraphITA 2011: Selected papers from the Workshop on Fundamentals and Applications of Graphene* (Springer, Berlin, Heidelberg) 2012, pp. 39–49.
[27] Goler S. *et al.*, *Carbon*, **51** (2013) 249.
[28] Riedl C., Coletti C. and Starke U., *J. Phys. D: Appl. Phys.*, **43** (2010) 374009.
[29] Ristein J., Mammadov S. and Seyller T., *Phys. Rev. Lett.*, **108** (2012) 246104.
[30] Mucha-Kruczyñski M., Tsyplyatyev O., Grishin A., McCann E., Fal'ko V. I., Bostwick A. and Rotenberg E., *Phys. Rev. B*, **77** (2008) 195403.
[31] Norimatsu W. and Kusunoki M., *Phys. Rev. B*, **81** (2010) 161410.
[32] Malard L. M., Nilsson J., Elias D. C., Brant J. C., Plentz F., Alves E. S., Castro Neto A. H. and Pimenta M. A., *Phys. Rev. B*, **76** (2007) 201401(R).
[33] Coletti C., Emtsev K. V., Zakharov A. A., Ouisse T., Chaussende D. and Starke U., *Appl. Phys. Lett.*, **99** (2011) 081904.
[34] Coletti C., Frewin C. L., Hoff A. M. and Saddow S. E., *Electrochem. Solid-State Lett.*, **11** (2008) H285.